Nuclear Engineering and Technology 54 (2022) 1508–1515

Contents lists available at ScienceDirect

Nuclear Engineering and Technology

journal homepage: www.elsevier.com/locate/net

Technical Note

The influence of the water ingression and melt eruption model on the MELCOR code prediction of molten corium-concrete interaction in the APR-1400 reactor cavity

Muritala A. Amidu*, Yacine Addad

Emirates Nuclear Technology Center (ENTC), Department of Nuclear Engineering, Khalifa University of Science and Technology, Post Office Box 127788, United Arab Emirates

ARTICLE INFO

Article history:
Received 26 April 2021
Received in revised form
6 August 2021
Accepted 29 September 2021
Available online 3 October 2021

Keywords:
Severe accident
MCCI
MELCOR code
APR1400 reactors
Water ingression model
Melt eruption model

ABSTRACT

In the present study, the cavity module of the MELCOR code is used for the simulation of molten corium concrete interaction (MCCI) during the late phase of postulated large break loss of coolant (LB-LOCA) accident in the APR1400 reactor design. Using the molten corium composition data from previous MELCOR Simulation of APR1400 under LB-LOCA accident, the ex-vessel phases of the accident sequences with long-term MCCI are recalculated with stand-alone cavity package of the MELCOR code to investigate the impact of water ingression and melt eruption models which were hitherto absent in MELCOR code. Significant changes in the MCCI behaviors in terms of the heat transfer rates, amount of gases released, and maximum cavity ablation depths are observed and reported in this study. Most especially, the incorporation of these models in the new release of MELCOR code has led to the reduction of the maximum ablation depth in radial and axial directions by ~38% and ~32%, respectively. These impacts are substantial enough to change the conclusions earlier reached by researchers who had used the older versions of the MELCOR code for their studies. and it could also impact the estimated cost of the severe accident mitigation system in the APR1400 reactor.

1. Introduction

During a postulated severe accident event, the integrity of the reactor pressure vessel is compromised, molten corium is relocated from the Reactor Pressure Vessel (RPV) to the reactor cavity. Attack on the concrete materials by the molten corium commonly referred to as Molten Corium Concrete Interaction (MCCI) could lead to the cavity Basemat Melt Through (BMT) situation where radioactive materials could be released into the environment. The safety analysis of this kind of accident scenario became much more important after the unfortunate 2011 Fukushima accident. In addition to the potential release of radioactive materials, a large amount of non-condensable and combustible gases are generated in the course of concrete decomposition by molten corium interaction. These gases could potentially raise the containment pressure and thereby compromise its integrity. However, owing to the limitation of experimental study of these phenomena due to severe temperature conditions, the use of computational code becomes inevitable and therefore, the reliability of such computational code has to be assured through the number of dominant phenomena captured using mechanistic models in such computational code.

For the ex-vessel stage of the severe accident progression, one of the prominent computational codes for the prediction of the MCCI is the cavity module (CAV package) of the MELCOR code which is essentially COCORN MOD-3 code with modification in the numerics and mechanistic models. Another common computational code for the prediction of the MCCI is the CORQUENCH code. One of the key distinguishing features of the above-mentioned computational codes are the mechanistic models for water ingression and melt eruption phenomena which were previously absent in the cavity module (CAV package) of MELCOR code but have been always present in CORQUENCH code. The motivation for this work is to investigate the retention of corium materials within the reactor cavity under MCCI condition for APR1400 with a focus on the analyses of the effect of the water ingression and melt eruption models on the heat transfer behavior during the MCCI especially in terms of the ablation depths of the cavity in both radial and axial

* Corresponding author.
E-mail addresses: amidu.alade@ku.ac.ae (M.A. Amidu), yacine.addad@ku.ac.ae (Y. Addad).

https://doi.org/10.1016/j.net.2021.09.036

directions. This way, it will be shown whether the incorporation of the CORQUENCH coolability models for water ingression and melt eruption into the cavity module of the MELCOR code, where it was missing, should be of serious concern.

2. Phenomenology and mathematical models

The molten corium concrete interaction is majorly a thermal process and can be regarded as quasi-steady for much of the period of the reactor accident. Thus, debris behavior and concrete ablation are represented by conservation energy with heat transfer relations as closure relations. There are two sources of heat in MCCI viz: decay heat from the debris and heat from chemical reactions in the concrete. One part of this heat is transferred to the top surface while the remaining part goes to the concrete floor. Heat flux to the concrete floor is used for the concrete decomposition, generation of water vapor and carbon dioxide, and melting of the residual oxide. The ablated concrete provides additional molten oxide and molten concrete from the reinforcing bars in the concrete to the debris pool. A more in-depth description of the complex processes involved in molten corium concrete interaction can be found in the cavity module (CAV package) reference manual of the MELCOR code [1,2]. However, detailed descriptions of the mathematical models of the two phenomena of interest (water ingression and melt eruption) are also provided in this study.

Based on the insight garnered from experimental observation, it was reported by Farmer et al. [3] that after crust formation, water can penetrate the debris by crack mechanisms to provide sufficient augmentation to the otherwise conduction-limited heat transfer process to remove decay heat. Three processes by which water could penetrate (shown in Fig. 1) into the debris have been identified through an experiment by Farmer et al. [3].

The first process is water ingression through interconnected porosity or cracks (Fig. 1). This process relies on crack propagation through the material, and as such is highly dependent upon the mechanical properties, since thermal stress is a key factor. The second process is particle bed formation through melt eruptions. In this case, concrete decomposition gases entrain melt droplets into the overlying coolant as they pass through the crust. The third process is the mechanical breach of a suspended crust where the thick crust that forms from water ingression could bond to the reactor cavity wall, eventually causing melt to separate from the crust as the MCCI continues downwards. The models for the first two processes (water ingression into the top crust, and the possibility of melt eruption through the top crust into the water to form an overlying layer) have been incorporated into the new release of MELCOR code version 2.2.18109. These two phenomena provide extra cooling for the molten debris.

2.1. Water ingression model

The water ingression model was adapted from the model developed by Epstein [4] which was based on the work of Lister [5] which bordered on the water ingression into molten lava. It has been observed in the OECD/MACE/MCCI experiments [6] that water can penetrate a crust through crevices present in the crust. This could effectively reduce the conduction zone in the crust. The water ingression model allows water into the crust layer based on the criterion that the top heat flux is less than a dry out heat flux (q''_{dry}). The dryout heat flux is defined as:

$$q''_{dry} = C_{dry}\left[\left(h_{lv}\frac{(\rho_l-\rho_v)g}{\nu_v}\right)^5\left(\frac{N_{dry}k_c^2\Delta e_{sat}^2}{c_p\Delta e_{cr}}\right)^4\right]^{1/13}[\alpha_T(T_{cr}-T_{sat})]^{15/13} \quad (1)$$

where q''_{dry}(W/m^2), C_{dry}, h_{lv}(J/kg), ρ_l(kg/m^3), ρ_v(kg/m^3), g(m/s^2), ν_v(m^2/s), N_{dry}(K-m$^{1/2}$), k_c(W/mK), Δe_{sat}(J/kg), c_p(J/kg-K), Δe_{cr}(J/kg), α_T(1/K), T_{cr}(K),and T_{sat}(K) represent the dryout heat flux, dimensionless empirical constant, heat of vaporization of water, the density of water, density of steam, gravitation constant, dynamic viscosity of steam, numerical constant, the thermal conductivity of crust, change in specific enthalpy from melt to saturation temperature, the specific heat capacity of melt, changes in specific enthalpy from crack temperature to saturation temperature, coefficient of thermal expansion for melt, crack temperature, and saturation temperature, respectively. The variables in Eq. (1) with their respective values or how they are computed are summarized in Table 1.

The material properties in the CAV package are those of the stand-alone CORCON code. They include internally consistent specific heats, enthalpies, and chemical potentials for a large number of condensed and gaseous species, based on fits to JANAF [12] and other data. All enthalpies are based on the JANAF thermochemical reference point. All heats of reaction are therefore implicitly contained in the enthalpy data. Also included are data on thermal expansivity and density, thermal conductivity, viscosity,

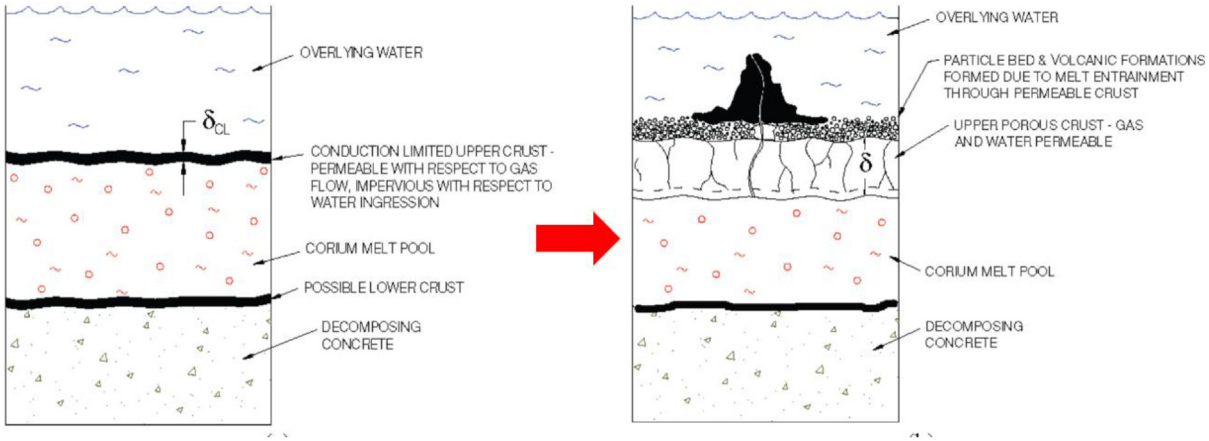

Fig. 1. Corium-concrete interaction with water ingression and melt eruption cooling mechanism [3].

Table 1
Definition of parameters of the water ingression model.

Variable Parameters	Description	Values
ρ_l (kg/m^3)	The density of water	960
h_{lv} (J/kg)	Heat of vaporization of water	Thermochemical table [12]
ρ_v (kg/m^3)	Density of steam	0.59
g (m/s^2)	Gravitation constant	9.8
ν_v (m^2/s)	Dynamic viscosity of steam	1.29×10^{-5}
N_{dry} (K-m$^{1/2}$)	Numerical constant	0.1
k_c (W/mK)	Thermal conductivity of crust	Thermochemical table [12]
Δe_{sat} (J/kg)	Change in specific enthalpy from melt to saturation temperature	Thermochemical table [12]
c_p(J/kg-K)	Specific heat capacity of melt	Mass-weighted averages of the constituent properties
α_T (1/K)	Coefficient of thermal expansion for melt	Mass-weighted averages of the constituent properties
Δe_{cr}(J/kg)	Change in specific enthalpy from crack temperature to saturation temperature	Thermochemical table [12]
T_{cr} (K)	Crack temperature	Computed using Eq. (2)
T_{sat} (K)	Saturation temperature	Thermochemical table [12]
σ_{tens} (Pa)	Tensile strength of the crust	6.77×10^7
E (Pa)	Young's modulus for the crust	1.25×10^{11}
T_s (K)	Melt solidus temperature	Mole-weighted combination of the solidus/liquidus temperatures of constituents
C_{dry}	Empirical constant	The reference manual does not give any value for the constant

and surface tension. The properties (specific heat capacity, thermal expansion coefficient … etc.) of the melt are mass-weighted averages of the constituent (Zr, ZrO_2, UO_2 … etc.) properties.

The mechanical properties (tensile strength, elastic modulus) are essential for estimating the crust dryout limit. Thus, the crack temperature is estimated using Eq. (2)

$$T_{cr} = T_s + \frac{\sigma_{tens}}{\alpha_T E} \tag{2}$$

According to Eq. (2), the crack temperature depends on the solidus temperature. Solidus and liquidus temperatures of corium–concrete mixtures depend on the composition of the mixture and are currently computed as the mole-weighted combination of the solidus/liquidus temperatures determined by considering every binary combination of material pairs in the mixture. The tensile strength of the crust $\sigma_{tens}(Pa) = 6.77\times 10^7$Pa, and Young's modulus for the crust $E = 1.25 \times 10^{11}$Pa. This water ingression model is implemented in the CAV package by adding a new crust layer to the CORCON model. This layer sits on top of the existing melt layer in CORCON and mass is transferred from the melt layer by a dynamic crust model which replaces the present static top crust model in the melt layer.

2.2. Melt eruption model

After the formation of a stable crust layer, the potential melt eruption phenomenon could provide enhancement of the molten debris cooling rate. By this process, melt droplets are entrained in the sparging concrete decomposition gases through the crust. The model is implemented in CAV by adding a new debris layer to the CORCON model. This layer sits on top of the new crust layer added for the water ingression model. Mass can be transferred to the debris layer through the crust from the melt layer via a melt ejection model. The entrained melts are then accumulated on the top surface of the crust and quenched by the overlying water pool. The melt eruption model is given by Eq. (3) and is used to capture the transfer of entrained melt from the debris, through the crust, to the upper surface of the crust. The rate of mass transfer is proportional to the gas sparging rate given by Eq. (3).

$$J_{melt} = K_{ent} J_{gas} \tag{3}$$

where J_{melt}(m/s), K_{ent}, and J_{gas}(m/s) represent the melt ejection rate, entrainment coefficient, and gas sparging rate. The entrainment coefficient (K_{ent}) is computed using the Ricou-Spalding correlation [7] which is defined by Eq. (4).

$$K_{ent} = E_{ent}\left(\frac{\rho_{gas}}{\rho_{melt}}\right)^{1/2} \tag{4}$$

where E_{ent}, ρ_{gas}(kg/m^3), and ρ_{melt}(kg/m^3) represent the user input entrainment constant (default value is 0.08), gas density, and melt density, respectively.

What determines the occurrence of the melt eruption is whether the gas velocity is higher than the minimum gas velocity (Eq. (5)) required to maintain active pores on the crust surface. This is applicable for a crust presumed to be floating on the melt

$$J_{min} = \frac{\kappa(\rho_c - \rho_m)g}{\mu_g} \tag{5}$$

where J_{min}(m/s), κ(m^2), ρ_c(kg/m^3), and μ_g(Pa-s), represent the minimum gas flow rate, crust permeability, crust density, and gas viscosity, respectively. The permeability is determined from the dryout heat flux using the correlation of Jones et al. [8] given by Eq. (6).

$$\kappa = \frac{2\mu_v q''_{dry}}{\rho_v h_{lv}(\rho_l - \rho_v)g} \tag{6}$$

This means that the permeability of the crust (if sufficient enough) determines whether to vent the gas flow from corium-concrete interaction through permeable structure under the applied pressure head by the overlying crust.

3. Problem description and input parameters for MCCI simulation

The APR1400 reactor cavity is designed to accommodate and evacuate heat from relocated core debris during a postulated severe accident. The large cavity flow area allows for a spreading of the core debris, thus enhancing its coolability within the reactor cavity region. The free volume of the cavity is ~963 m^3, and the cavity floor comprises an area of ~80 m^2 that is available for corium spreading [9]. For the APR1400 concrete, the concrete composition is close to SIL or CORCON-I concrete. The previous MELCOR simulation of

severe accident progression in APR1400 for a large-break loss-of-coolant accident by Lim et al. [10] is selected as a base case in this study. In this study, the Lim et al. [10] simulation data is recalculated with a stand-alone cavity module of the MELCOR code with the assumptions that neither action of depressurization nor flooding of the cavity for ex-vessel cooling is taken to contain the molten corium within the reactor pressure vessel. Thus, the melt is expected to be released at about 10,000 s (following the reactor scram) from the lower plenum of the reactor pressure vessel to the cavity. It is further assumed that 100% of the molten debris materials present in the reactor pressure vessel, relocate to the reactor cavity. The predicted masses of the composition of the molten debris are shown in Table 2. For the nominal reactor operating power of 4666 MW_{th}, the molten corium that relocated to the cavity after 10,000 s has an initial temperature of 2843 K (see Lim et al. [10]) and subsequent decay heat is modeled according to ANS 79 decay heat curve. The input parameters of the cavity module (CAV package) of the MELCOR code for APR1400 are summarized in Table 3 and the modeling options selected for phenomena present in the MCCI are also summarized in Table 4.

A typical model of reactor cavity in MELCOR code is shown in Fig. 2 where RW, RAD, HIT, and HBB represent the cavity outer radius, inner radius, axial depth, and axial wall thickness, respectively. The geometry of the reactor cavity wall is cylindrical and a number of body points along the cavity wall can be set so that heat flux to concrete at these body points can be used to compute the local ablation rate as shown in Fig. 2(a). A total of 95 body points are used in this study with 30 body points at the bottom wall, 10 body points defining the corner, and 55 body points at the radial wall of the cavity. Concrete ablations result in newly calculated positions of the body points. Therefore, the concrete ablation depth can be computed using the change of positions of the body point where concrete ablates. Additionally, the physical system considered by cavity models in MELCOR consists of an axisymmetric concrete cavity, a multilayered debris pool, and a set of boundary conditions provided by control volume hydrodynamic (CVH) at the top surface of the debris as can be seen in Fig. 2(b). Based on the APR1400 design parameters, the input parameters representing the shape of the cavity: RW, RAD, HIT, and HBB are 7.557 m, 5.057 m, 12 m, and 2.5 m, respectively.

4. Discussion of results and conclusion

The water ingression model has been previously validated in MELCOR/CORCON-MOD3 code by Sevon [13] against CCI-2 and CCI-3 experimental data as shown in Fig. 3. The water ingression model gave a good prediction of the CCI-2 experimental data with only 9% underestimation of the cumulative steam flow rate. However, for the CCI-3 experiment the water ingression model overestimated the coolability by 45%. The effect of the water ingression model on the predicted concrete ablation cannot be compared with the experimental data because flooding had little effect on ablation in CCI experiments since the experiments ended soon after the vessel was flooded. The default heat transfer parameters of the MELCOR/CORCON-MOD3 code without water ingression include the multiplication of the boiling heat transfer coefficient by 10 and the thermal conductivity of oxides and metals by 5. These multipliers were supposed to account for water ingression enhancement, but the users' guide [2] emphasizes that these multipliers are parametric control, not models.

Table 2
Molten corium composition from Lim et al. [10] and Amidu et al. [11].

Constituent Materials	Mass [kg]
UO_2	120000
ZrO_2	100000
Zr	20000
FeO	6000
Fe	3000
Cr	1000

Table 3
Summary of the input parameters for APR1400.

Parameter	Values
Corium mass, kg	187,000
Cavity radius, m	5.057
Cavity area, m^2	80.36
Initial corium temperature, K	2843
Time after scrams, sec	10,000
System pressure, MPa	0.1
Coolant mass, kg	577,000
Coolant flooding time, sec	10,000
Coolant temperature, K	373 (saturated)
Concrete type	CORCON-I
Concrete density, kg/m^3	2340
Initial concrete temperature, K	300
Concrete solidus temperature, K	1350
Concrete liquidus temperature, K	1650
Concrete ablation temperature, K	1450

The incipience of the water ingression into the crust is indicated by the condition that the dryout heat flux (predicted by Eq. (1)) is greater than the crust's upper surface heat flux. This condition is met throughout right from the beginning but becomes noticeable after about 2500 s as shown in Fig. 4(a). Also, Fig. 4(b) shows the evolution of the crust (in terms of its mass) which becomes fully formed and stable at about 7500 s. The additional heat transfer associated with the water ingression mechanism is also shown in Fig. 4(a) which is an improvement over the conduction-limited heat transfer presents in a situation when the water ingression phenomenon is not considered. This augmentation of the heat transfer (extra cooling effect) is reflected in the upper surface temperature of the crust as can be seen in Fig. 4(c) where the upper surface temperature of the crust with the water ingression model is lower than that without water ingression model. On the contrary, following the stable crust formation, the melt eruption phenomenon does not occur because the integral superficial gas velocity (J_{gas}) is not up to the minimum gas velocity (J_{min}) thereby producing a zero for the superficial gas velocity of the entrained melt (J_{melt}) into the overlying water pool as shown in Fig. 4(d). Thus, melt eruption cooling is nonexistent under the severe accident condition of APR1400 simulated in this study.

Interestingly, the fraction of the decay heat and chemical reaction heat removed through the water ingression phenomenon results in the reduction of the heat loss to the concrete and heat loss to the water pool as can be seen in Fig. 5(a). The accompanying effect of the presence of water ingression phenomenon during molten-corium concrete interaction is the substantial reduction of the ablation depth as depicted by the cavity profile shown in Fig. 5(b). This explains the disparity between MELCOR and CORQUENCH codes in terms of the predicted ablation depth which was earlier observed by Park et al. [9]. Besides, Fig. 5(c) indicates that the water ingression phenomenon also causes a significant reduction in the amount (mass) of water vapor (H_2O) and carbon dioxide (CO_2) gases released to the containment environment. There is no difference in the amount of the hydrogen (H_2) and carbon monoxide (CO) gases released with and without water ingression and melt eruption models. This is because these gases (H_2 and CO) come from the oxidation of metals in the debris, unlike water vapor (H_2O) and carbon dioxide (CO_2) that come from the decomposition of the

Table 4
Summary of modeling assumption in the cavity package of MELCOR code.

Phenomena	Modeling options
Melt-concrete heat transfer model	Bradley slag film model
Debris layering and mixing	Enforced complete mixing (Homogeneous)
Upward heat transfer	1. Convection (by air) 2. Thermal radiation 3. Boiling curve (if water is present)
Heat generation	1. Decay heat 2. Chemical reaction
Ablation model	Quasi-steady
Void fraction	Brockmann correlations
Melt solid fraction	Linear interpolation of Melt solidus and liquid temperature
Solids impact on viscosity	Kunitz model
Available geometry	2-D all bodies including 2-D cylinder

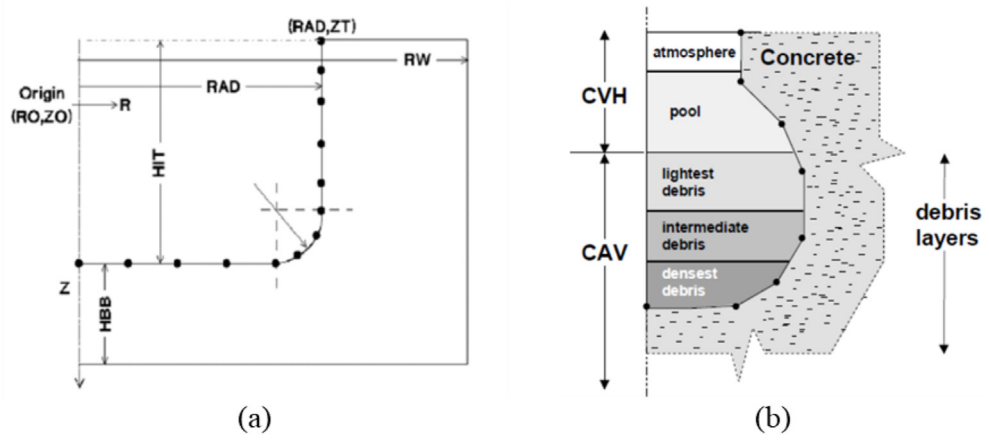

Fig. 2. (a)Shape of reactor cavity, and (b) schematic of the debris layers used in MELCOR simulation [1].

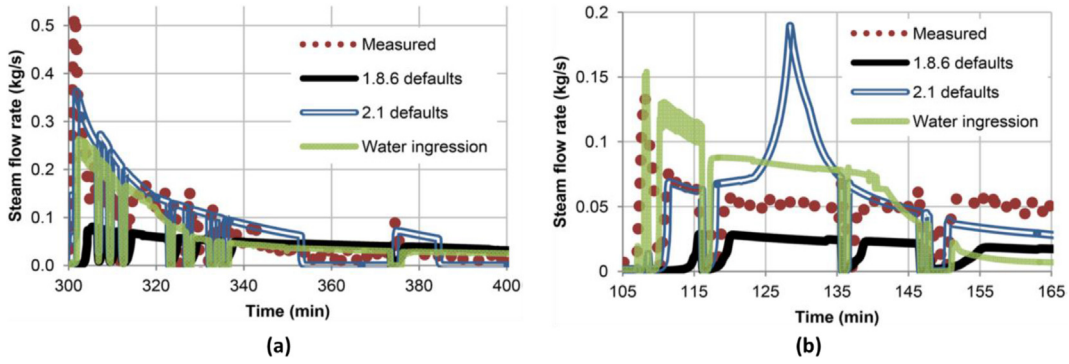

Fig. 3. Validation of water ingression model by Sevon [11]: (a) CCI-2; (b) CCI-3 experiments.

concrete under the thermal load of the molten corium. Thus, the coolability enhancement introduced by the water ingression and melt eruption model slows down the decomposition of the concrete, hence the reduction of the amount of water vapor (H_2O) and carbon dioxide (CO_2) released. Whereas this coolability enhancement does not affect the amount of Hydrogen (H_2) gas and carbon monoxide (CO) gas. The comparison between the predicted maximum ablation depths (shown in Fig. 5(d)) of the cavity with the presence and absence of water ingression phenomena shows that the maximum ablation depth in radial and axial directions get reduced by ~38% and ~32%, respectively when the water ingression model is used. Further reduction of these parameters could have taken place had it been that the melt eruption phenomenon also occurred.

Moreover, to check the influence of the thermal resistance between the melt and the concrete on the prediction of the concrete ablation considering the water ingression and melt eruption models, the gas film model is considered in addition to the slag film model earlier used (see Table 2) for the melt-concrete heat transfer process. The gas film model assumes that the debris is separated from the concrete by gas film and the heat transfer process is analogous to either the Taylor-instability-bubbling film boiling or attached-flow film boiling depending on the inclination. In contrast, the Bradley slag film model was developed based on the transient growth and removal of debris. However, the prediction of the concrete ablation using the slag film model slightly deviates from that of the gas film

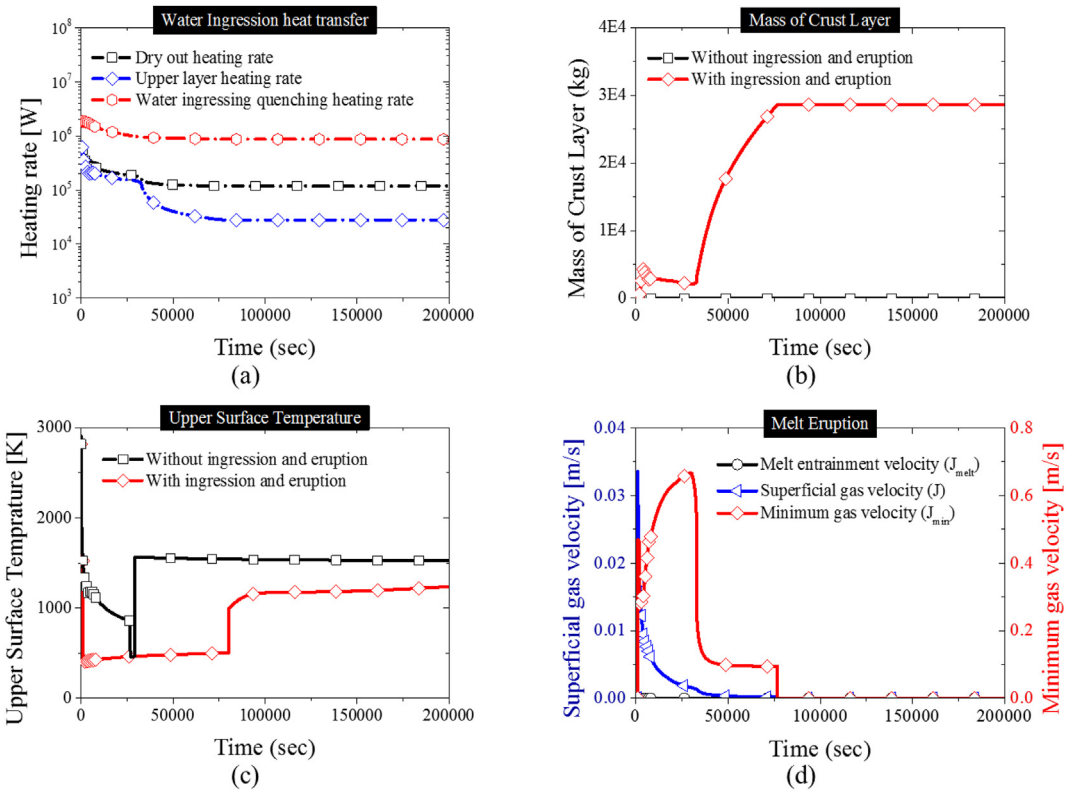

Fig. 4. (a) Water ingression parameters, (b) Mass of crust layer, (c) Upper crust surface temperature, and (d) Melt eruption parameters.

model as can be seen in Fig. 6(a). The slag film model predicts higher ablation depth in the radial direction while the gas film model predicts high ablation in the axial direction Also, a 2-layer (oxide layer and metallic layer) pool mixing modeling option has been considered in contrast to earlier used single-layer homogeneous mixing modeling option (see Table 2). The separation of the melt does not have a substantial effect on the ablation of the concrete as can be seen in Fig. 6(b). Model for the stratification of layers causes lower ablation in the radial direction while the homogeneous mixing gives lower ablation in the axial direction.

5. Conclusion

This work tests the water ingression and melts eruption models that are newly added to the MELCOR code. Previously, Sevon [13] had shown that the water ingression model performed satisfactorily against CCI experimental data [14] that involved the release of gas bubbles from the concrete to the melt. The melt coolability of the CCI-2 experiment was reported to be predicted well while that of CCI-3 was somewhat overpredicted. However, the validation of the water ingression and melt eruption models in terms of the ablation rate of the concrete could not be performed. This is because the CCI experiments were conducted with late flooding and high concrete content in the melt at the flooding time. It would have been insightful to validate the water ingression and melt eruption model against MCCI experiments with early flooding but no suitable experiment was found. Thus, more suitable experimental work is required for the detailed validation of these new coolability models. Nonetheless, the impact of these new models on the ablation rate of the reactor cavity of APR1400 reactors under a severe accident condition initiated by the late phase of postulated large break loss of coolant (LB-LOCA) is performed in this study.

Thus, a MELCOR code ver. 2.2.18019 which includes the implementation of the new water ingression and melt eruption models in the cavity package is used for the simulation of the MCCI behavior of the APR1400 reactor cavity during the late phase of postulated severe accident scenario. Significant changes in the MCCI behaviors in terms of the heat transfer, amount of gases released, and maximum cavity ablation depths are observed and reported in this study. Specifically, the amount of water vapor and carbon dioxide gases released are substantially increased while the concrete ablation depths in both the radial and axial directions are noticeably reduced. These changes are substantial enough to change the conclusions earlier reached by researchers who had used the old versions of the MELCOR code which do not have water ingression and melt eruption model for their studies. The implementation of these two models in the cavity module of the MELCOR code essentially changes the previous assumption in the older version of the MELCOR code that the crust layer is only permeable to gases produced by the decomposition of the concrete. This implies that the crust is not only permeable to the released gases from concrete decomposition but also water and entrained melt. The implementation of this kind of mechanistic model in the MELCOR code is essential for its paradigm shift from parametric models to ensure the best estimation from the code and this would further reduce the uncertainties in the code.

Declaration of competing interest

The authors declare that they have no known competing

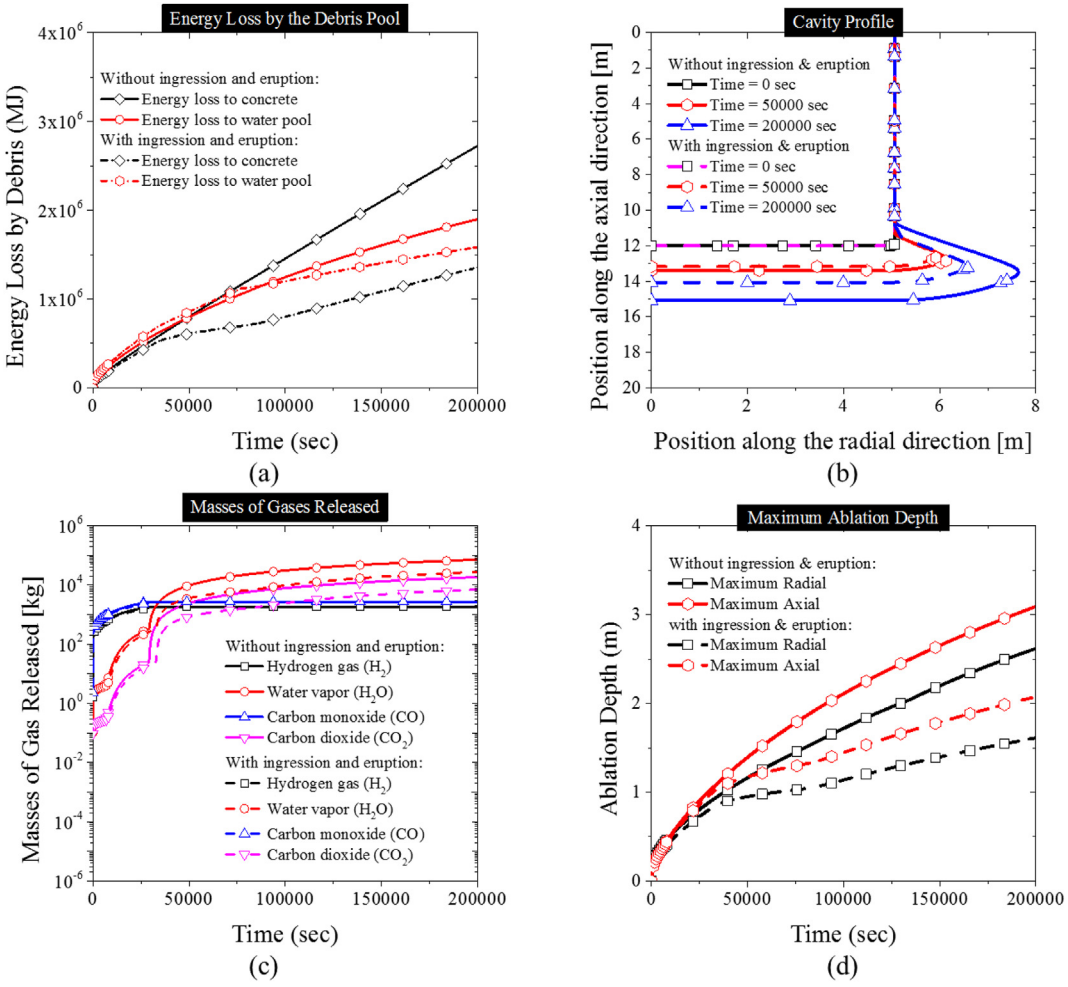

Fig. 5. (a) Energy loss by debris pool, (b) Cavity profile, (c) Masses of gas released, and (d) Maximum ablation depths.

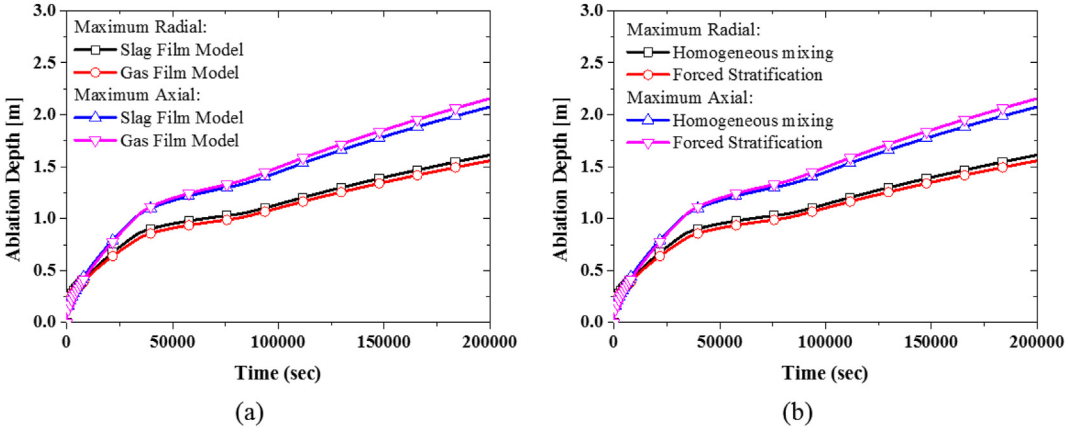

Fig. 6. (a) Effect of the melt-concrete interface heat transfer model, (b) Effect of the melt mixing assumptions.

financial interests or personal relationships that could have appeared to influence the work reported in this paper.

References

[1] L.L. Humphries, B.A. Beeny, F. Gelbard, T. Haskin, D.L. Louie, J. Phillips, R.C. Schmidt, N.E. Bixler, in: MELCOR Computer Code Manuals vol. 1, Primer and User's Guide, 2021. SAND2021-0252.

[2] L.L. Humphries, B.A. Beeny, F. Gelbard, T. Haskin, D.L. Louie, J. Phillips, R.C. Schmidt, N.E. Bixler, in: MELCOR Computer Code Manuals vol. 2, Reference Manual, 2021. SAND2021-0241.

[3] M.T. Farmer, D.J. Kilsdonk, R.W. Aeschlimann, Corium coolability under ex-vessel accident conditions for LWRs, Nucl. Eng. Technol. 4 (No. 5) (2009) 575–602.

[4] M. Epstein, Dryout heat flux during penetration of water into solidifying rock, J. Heat Tran. 128 (2006) 847.

[5] C.R. Lister, On the penetration of water into hot rock, Geophys. J. Roy. Astron. Soc. 39 (1974) 465.

[6] M.T. Farmer, et al., Status and future direction of the melt attack and coolability experiments (MACE) program at argonne national laboratory, in: Proceedings 9th Int. Conf. on Nucl. Eng., Nice, France, April 8-12, 2001.

[7] F.B. Ricou, D.B. Spalding, Measurement of entrainment of axisymmetrical turbulent jets, J. Fluid Mech. 11 (1961) 21.

[8] S.W. Jones, et al., Dryout heat fluxes in particulate beds heated through the base, J. Heat Tran. 106 (1984) 176.

[9] J.-H. Park, H.Y. Kim, S.W. Hong, K.S. Ha, MCCI Simulations for APR-1400 Total Loss of Main Feed Water Sequence, Transactions of the Korean Nuclear Society, Spring Meeting, Taebaek, Korea, 2011. May 26-27.

[10] K. Lim, Y. Cho, S. Whang, H.S. Park, Evaluation of an IVR-ERVC strategy for a high power reactor using MELCOR 2.1, Ann. Nucl. Energy (2017) 337–349.

[11] M.A. Amidu, Y. Addad, J.I. Lee, D.H. Kam, Y.H. Jeong, Investigation of the pressure vessel lower head potential failure under IVR-ERVC condition during a severe accident scenario in high power reactors, Nucl. Eng. Des. 376 (2021), 11107.

[12] JANAF Thermochemical Tables, DOW Chemical Company, Thermal Research Laboratory, Midland, MI, 1965.

[13] T. Sevon, Modeling of water ingression mechanism for corium cooling with MELCOR, Nucl. Technol. 197 (2017) 171–179.